Downloaded from rspa.royalsocietypublishing.org on July 13, 2012

PROCEEDINGS OF THE ROYAL SOCIETY A MATHEMATICAL, PHYSICAL & ENGINEERING SCIENCES

Disintegration of Water Drops in an Electric Field

Geoffrey Taylor

Proc. R. Soc. Lond. A 1964 **280**, 383-397
doi: 10.1098/rspa.1964.0151

References

Article cited in:
http://rspa.royalsocietypublishing.org/content/280/1382/383#related-urls

Email alerting service

Receive free email alerts when new articles cite this article - sign up in the box at the top right-hand corner of the article or click **here**

To subscribe to *Proc. R. Soc. Lond. A* go to: **http://rspa.royalsocietypublishing.org/subscriptions**

Downloaded from rspa.royalsocietypublishing.org on July 13, 2012

Disintegration of water drops in an electric field

By Sir Geoffrey Taylor, F.R.S.

(*Received* 21 *February* 1964)

[Plates 22 to 24]

The disintegration of drops in strong electric fields is believed to play an important part in the formation of thunderstorms, at least in those parts of them where no ice crystals are present. Zeleny showed experimentally that disintegration begins as a hydrodynamical instability, but his ideas about the mechanics of the situation rest on the implicit assumption that instability occurs when the internal pressure is the same as that outside the drop. It is shown that this assumption is false and that instability of an elongated drop would not occur unless a pressure difference existed. When this error is corrected it is found that a drop, elongated by an electric field, becomes unstable when its length is 1·9 times its equatorial diameter, and the calculated critical electric field agrees with laboratory experiments to within 1 %.

When the drop becomes unstable the ends develop obtuse-angled conical points from which axial jets are projected but the stability calculations give no indication of the mechanics of this process. It is shown theoretically that a conical interface between two fluids can exist in equilibrium in an electric field, but only when the cone has a semi-vertical angle 49·3°.

Apparatus was constructed for producing the necessary field, and photographs show that conical oil/water interfaces and soap films can be produced at the calculated voltage and that their semi-vertical angles are very close to 49·3°. The photographs give an indication of how the axial jets are produced but no complete analytical description of the process is attempted.

Introduction

The distortion and bursting of water drops in an electric field has formed the subject of a number of experimental researches. The practical interest of the subject is that it seems to be an important factor in the production of thunderstorms at any rate in those parts of them where it is too warm for ice crystals to exist. Zeleny (1917) photographed drops held at the end of capillary tubes and raised to a high potential. He measured the potential at which they disintegrated owing to the formation of a pointed end from which issued a narrow jet. Figure 1, plate 22, which is reproduced from Zeleny (1917), shows a jet of glycerine formed in this way. When water was used the end of the drop vibrated violently.

Wilson & Taylor (1925) found that a similar phenomenon occurs when an uncharged soap bubble is subjected to a uniform electric field. Macky (1931) and Nolan (1926) showed that the same kind of disintegration occurs when a drop of water falls between parallel plates when a potential gradient is maintained between them. Zeleny showed experimentally that the disintegration is due to instability rather than the formation of ionic currents and he concluded, on dimensional grounds, that the criterion of instability must be of the form

$$V^2/r_0 T = C, \tag{1}$$

where V is the potential, r_0 the radius of the drop, T surface tension and C a constant. His results were in fact well presented by taking $C = 140$ when V was expressed in electrostatic units.

The Royal Society is collaborating with JSTOR to digitize, preserve, and extend access to
Proceedings of the Royal Society of London. Series A, Mathematical and Physical Sciences.
www.jstor.org

Downloaded from rspa.royalsocietypublishing.org on July 13, 2012

Wilson & Taylor (1925) found that a soap bubble in an electric field F becomes unstable when $Fr_0^{\frac{1}{2}} = 3670 \pm 100\,\mathrm{V\,cm^{-\frac{1}{2}}}$. The variation $\pm 100\,\mathrm{V}$ represents the standard deviation in eight groups of measurements in which r_0 varied from 0·25 to 1·06 cm expressed in a form analogous to (1) and using the measured value of the surface tension of the soap solution used ($T = 2 \times 29 = 58\,\mathrm{dyn/cm}$). Wilson & Taylor's result, expressed in electrostatic units, is

$$F(r_0/T)^{\frac{1}{2}} = 1{\cdot}61 \pm 0{\cdot}04. \tag{2a}$$

Macky's measurements with water drops are represented by

$$F(r_0/T)^{\frac{1}{2}} = 1{\cdot}51. \tag{2b}$$

The equations representing the equilibrium of a deformed drop under the action of surface tension and an electric field can be set up and the shape of the drop could be determined if a solution could be obtained. This, however, has not yet been done by any worker in this field except when the distortion from the spherical form is small.

In the absence of analysis of this kind Zeleny (1915) assumed that the drop in his experiments became elongated approximately into the form of a prolate spheroid. The intensity of the field at the poles of a spheroid of constant volume can be calculated and the resulting stress normal to its surface found. As the length of the spheroid increases this stress increases and Zeleny tried to use this fact to find a criterion of stability. His method was based on Rayleigh's (1882) calculation of the limiting charge, Q, which an isolated drop of radius r_0 can hold before it becomes unstable. Rayleigh's result was that when $Q^2 > 4\pi r_0^3 T(n+2)$ the drop becomes unstable for a displacement proportional to the Legendre function $P_n(\cos\theta)$, provided $n \geqslant 2$. When $Q^2 < 16\pi r_0^3 T$ or the potential $V < (16\pi r_0 T)^{\frac{1}{2}}$, the drop is stable for all displacements, and when V first exceeds this value the drop becomes unstable only for the disturbance $P_2(\cos\theta)$ for which it becomes slightly ellipsoidal while the displacement is small.

Zeleny's method for adapting Rayleigh's stability criterion for a charged sphere so as to be applicable to a spheroid was to assume that it applies at the polar end when Rayleigh's r_0 is replaced by the polar radius of curvature of the spheroid and the mechanical stress due to the electric field (which can be calculated for a spheroid) is the same as that on the sphere when it becomes unstable. It seems that this method, though it has been accepted by later workers, is unsound because it takes no account of the fact that the pressure inside the spheroid is not in general the same as that outside when instability occurs. In Zeleny's equations the symbol p, representing this difference, appears in the equation of equilibrium but the pressure is assumed to vanish when the drop becomes unstable, in fact it is really this assumption which is the basis of Zeleny's criterion rather than Rayleigh's criterion for the stability of a charged sphere. The confusion probably arose because when an isolated drop is charged to Rayleigh's critical potential for unstable displacements proportional to $P_n(\cos\theta)$ the internal pressure happens to be equal to the external pressure when $n = 2$. This accidental circumstance only occurs when $n = 2$ and the spherical drop begins to become spheroidal. It does not occur for other values of n, or, as will

Downloaded from rspa.royalsocietypublishing.org on July 13, 2012

be shown later, when a spheroid of finite eccentricity becomes unstable in a uniform electric field. It is not surprising therefore that Zeleny's method is not successful as a guide to understanding the mechanics of the instability in spite of the fact that photographs of drops and soap films in a uniform electric field show them to be nearly spheroidal before they disintegrate.

Spheroidal approximations

Though the equations of equilibrium cannot be completely satisfied over the surface of a freely charged spheroid or a spheroid in a uniform field unless the ellipticity is small, the fact that a soap film in an electric field is nearly spheroidal makes it worthwhile to find out how nearly the equilibrium conditions can be satisfied. Two approximations (I and II) will be considered. In I the equilibrium equations will be satisfied at the poles and the equator. In II they are satisfied at the poles, but at the equatorial section the balance between the internal pressure, surface tension and total force due to the electric field acting over one-half of the spheroid is satisfied. If the equilibrium equations had been satisfied at all points of the spheroidal surface the two approximations I and II would have given identical results. The difference between them is an indication of the error involved in the spheroidal approximation.

Stress on a spheroid due to the electric field

The electric field round an isolated spheroid charged to potential V and also that due to a spheroid in a uniform electric field of strength F can be calculated by methods described in text books (e.g. Jeans 1915). Taking the equation to the axial section of a prolate spheroid as $x^2/a^2+y^2/b^2 = 1$, where a is the major axis, the ellipticity is $e = (1-a^2/b^2)^{\frac{1}{2}}$. For the spheroid charged to potential V the electric field at the surface of any point is

$$\frac{\mathrm{d}V}{\mathrm{d}n} = \frac{PV}{b^2 I_1}, \tag{3}$$

where P is the perpendicular from the centre of the spheroid onto the tangent plane at the point in question and

$$I_1 = \frac{1}{2e}\ln\left(\frac{1+e}{1-e}\right). \tag{4}$$

Since $P^2 = b^2(1-x^2e^2/a^2)^{-1}$ the normal stress at the point x is

$$\widehat{nn} = \frac{1}{8\pi}\left(\frac{\mathrm{d}V}{\mathrm{d}n}\right)^2 = \frac{V^2}{8\pi b^2(1-x^2e^2/a^2)\,I_1^2}. \tag{5}$$

For the uncharged spheroid in a uniform field, F, parallel to the major axis

$$\frac{\mathrm{d}V}{\mathrm{d}n} = \frac{FxP}{b^2 I_2}, \tag{6}$$

where

$$I_2 = \frac{1}{2e^3}\ln\frac{1+e}{1-e} - \frac{1}{e^2}. \tag{7}$$

The stress is perpendicular to the surface and equal to

$$\widehat{nn} = \frac{1}{8\pi}\frac{F^2x^2}{b^2(1-x^2e^2/a^2)\,I_2^2}. \tag{8}$$

Downloaded from rspa.royalsocietypublishing.org on July 13, 2012

Approximate equilibrium equations

The discontinuity of normal stress due to surface tension is $T(r_1^{-1}+r_2^{-1})$ where r_1 is the radius of curvature of the ellipse $x^2/a^2+y^2/b^2 = 1$ and r_2 is the other principal radius of curvature of the spheroid. The analytical expressions for r_1 and r_2 are

$$r_1 = a^2b^2\left(\frac{x^2}{a^4}+\frac{y^2}{b^4}\right)^{\frac{3}{2}}, \quad r_2 = b^2\left(\frac{x^2}{a^4}+\frac{y^2}{b^4}\right)^{\frac{1}{2}}. \tag{9}$$

At the end of the major axis $r_1^{-1}+r_2^{-1} = 2ab^{-2}$, and at the end of the minor axis $r_1^{-1}+r_2^{-1} = ba^{-2}+b^{-1}$. In approximation I the equations of equilibrium are

$$2ab^{-2}T-p = (\widehat{nn})_{x=a} \tag{10}$$

and

$$T(ba^{-2}+b^{-1})-p = (\widehat{nn})_{x=0}, \tag{11}$$

where p is the difference between the internal and external pressures. In approximation II (10) is retained unaltered but (11) is replaced by

$$2\pi bT-\pi b^2p = 2\pi\int_0^b \widehat{nn}y\,\mathrm{d}y. \tag{12}$$

Eliminating p, approximation I yields

$$T(2ab^{-2}-ba^{-2}-b^{-1}) = (\widehat{nn})_{x=a}-(\widehat{nn})_{x=0} \tag{13}$$

and II yields

$$\begin{aligned} T(2ab^{-2}-2b^{-1}) &= (\widehat{nn})_{x=a}-2b^{-2}\int_0^b \widehat{nn}y\,\mathrm{d}y \\ &= (\widehat{nn})_{x=a}-2a^{-2}\int_0^a \widehat{nn}x\,\mathrm{d}x. \end{aligned} \tag{14}$$

Since the drop has constant volume a and b must be expressed in terms of r_0, the original radius of the drop. Writing $\alpha = 1-e^2$, we have

$$a = r_0\alpha^{-\frac{1}{3}}, \quad b = r_0\alpha^{\frac{1}{6}}. \tag{15}$$

For the charged spheroid

$$(\widehat{nn})_{x=a} = \frac{V^2}{8\pi r_0^2 I_1^2}\alpha^{-\frac{4}{3}}, \quad (\widehat{nn})_{x=0} = \frac{V^2\alpha^{-\frac{1}{3}}}{8\pi r_0^2 I_1^2}. \tag{16}$$

Approximation I for the charged spheroid is

$$V(\pi r_0 T)^{-\frac{1}{2}} = N(\alpha)\,I_1, \tag{17}$$

where

$$[n(\alpha)]^2 = 8\alpha^{\frac{2}{3}}(2-\alpha^{\frac{1}{2}}-\alpha^{\frac{3}{2}})/(1-\alpha). \tag{18}$$

For the spheroid in a uniform field F, approximation I is

$$Fr_0^{\frac{1}{2}}T^{-\frac{1}{2}} = (8\pi)^{\frac{1}{2}}M(\alpha)\,I_2, \tag{19}$$

where

$$M(\alpha) = \alpha^{\frac{2}{3}}(2-\alpha^{\frac{1}{2}}-\alpha^{\frac{3}{2}})^{\frac{1}{2}},$$

and II is

$$F^2r_0T^{-1} = 16\pi\alpha^{\frac{5}{6}}(\alpha^{-\frac{1}{2}}-1)\,I_2^2/\phi(e)$$

and

$$\phi(e) = \left[\frac{1}{1-e^2}+\frac{1}{e^4}\{e^2+\ln(1-e^2)\}\right]. \tag{20}$$

Downloaded from rspa.royalsocietypublishing.org on July 13, 2012

Accuracy of the spheroidal approximations

The calculated relation for the isolated spheroid between $V(\pi r_0 T)^{-\frac{1}{2}}$ and a/b according to approximation I is shown in figure 2. For the uncharged spheroid the relationship between $Fr_0^{\frac{1}{2}}T^{-\frac{1}{2}}$ and a/b, according to I, is shown in figure 3. Approximation II is so close to I that it is only in one part of the curve that the difference reaches about 1 % and can be shown in figure 3. The closeness of the two approximations suggested that the difference between the true form of the interface and the spheroidal approximation must be very small. The difference between the normal force due to pressure and surface tension and that due to electric field was therefore

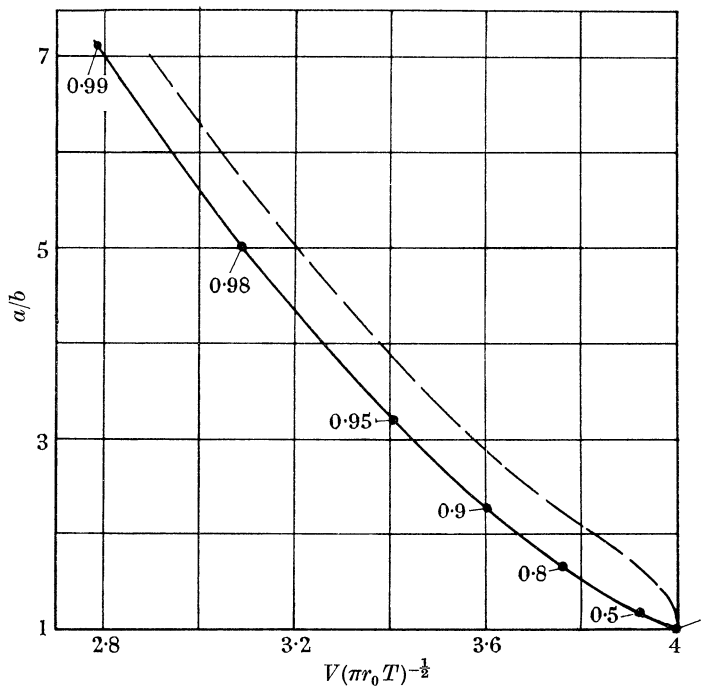

FIGURE 2. Charged spheroid. Broken curve shows Zeleny's criterion.

calculated for approximation I. Here the conditions assumed were that the equilibrium equations are satisfied at the equator and the poles. The error of the spheroidal approximation can therefore be appreciated by calculating the difference between the electric and mechanical stress at intermediate points.

If we write $x/a = \xi$, $y/b = (1-\xi^2)^{\frac{1}{2}}$ and $b^2/a^2 = \alpha$, (9) becomes

$$\frac{1}{r_1}+\frac{1}{r_2}=\frac{1}{a}\left\{\frac{1-\alpha^{-1}-\xi^2(\alpha^{-1}-1)}{\alpha^2[\alpha^{-1}-\xi^2(\alpha^{-1}-1)]}\right\}. \tag{21}$$

The mechanical stress due to the electric field is proportional to x^2p^2 or to

$$\frac{\xi^2}{\alpha^{-1}-\xi^2(\alpha^{-1}-1)}. \tag{22}$$

Downloaded from rspa.royalsocietypublishing.org on July 13, 2012

For the comparison between the two it is necessary to multiply one of them by a factor to bring the difference between the values at $\xi = 0$ and $\xi = 1$ to equality (this is equivalent to determining $Fr_0^{\frac{1}{2}}T^{-\frac{1}{2}}$ using approximation I).

Numerical comparison

For a numerical comparison the calculation was carried out for the case $a/b = 2$ which is close to the limiting value for stable equilibrium. In this case $\alpha^{-1} = 4$.

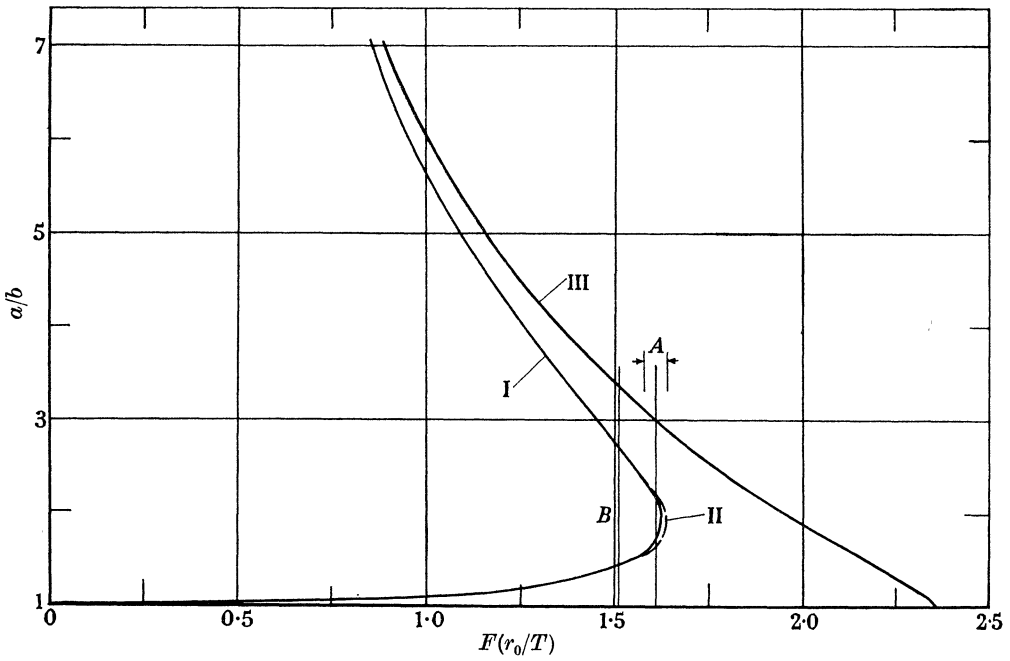

FIGURE 3. Uncharged drop in uniform field. I and II according to approximations I and II. *A*, Wilson & Taylor's measurements. *B*, Macky's measurements. III, Zeleny's criterion for stability.

It is convenient to express the normal stresses as fractions of the value of $\widehat{nn}$ at the poles. In these units (22) gives the stress at ξ due to the electric field as

$$p_E = \frac{\xi^2}{4-3\xi^2}, \tag{23}$$

and since the stress due to the surface tension is proportional to $r_1^{-1}+r_2^{-1}$, (21) becomes

$$p_T = B(5-3\xi^2)(4-3\xi^2)^{-\frac{3}{2}}, \tag{24}$$

and according to approximation I, B must be chosen so that the difference between the values of p_T at $\xi = 0$ and $\xi = 1$ is 1·0 so that $B = 8/11$.

The equilibrium equation, if it could be satisfied would be

$$p_E = p_T - p_p, \tag{25}$$

where p_p is the pressure expressed in the same units as p_E and p_T. Evidently $p_p = \frac{8}{11}(\frac{5}{8}) = \frac{5}{11}$. The values of p_E and $p_T - p_p$ calculated from (23) and (24) are

Downloaded from rspa.royalsocietypublishing.org on July 13, 2012

shown in figure 4, but the ordinates are $y/b = (1-\xi^2)^{\frac{1}{2}}$ instead of ξ because this choice reveals the error in (25) more clearly. It will be seen that the error is surprisingly small, amounting to 2·0 % at its maximum when $y/b \sim 0{\cdot}5$. In figure 4, $-p_p$ is shown in order to reveal the large part that the internal pressure plays in the equilibrium equation and therefore in the stability condition.

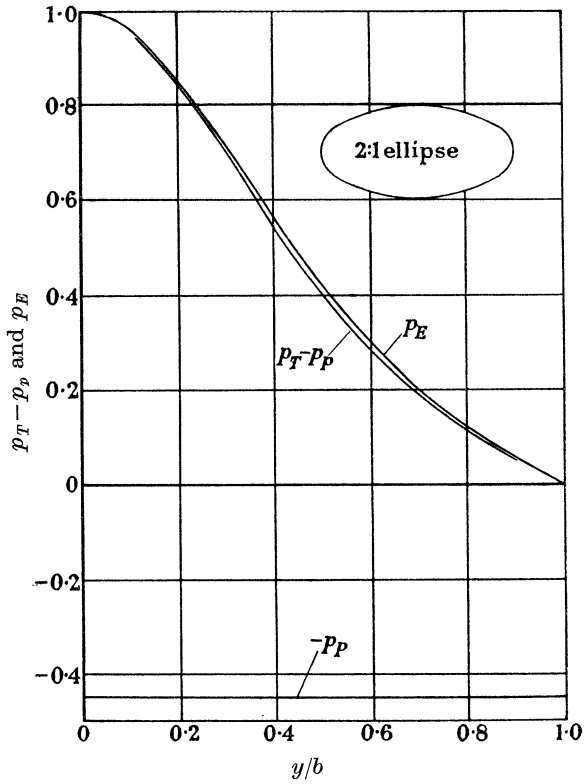

FIGURE 4. Distribution of stresses due to electric field p_E, surface tension p_T, internal pressure p_p for case $a/b = 2$.

COMPARISON WITH OBSERVATIONS

Isolated drop at constant potential V

Equation (17) gives the equilibrium configurations at which, according to approximation I, an isolated spheroidal drop, raised to potential V, could be in equilibrium with its own electric field. The relation between $V(\pi r_0 T)^{-\frac{1}{2}}$ and a/b according to approximation I is shown in figure 2. Since there is no stationary value for V as a/b increases, the only stable equilibrium condition is when the drop is spherical and $V(\pi r_0 T)^{-\frac{1}{2}} < 4$. This is Rayleigh's criterion. Thus there can be no criterion of stability of the type envisaged by Zeleny for isolated drops. The instability which Zeleny observed when drops were already elongated at a definite value of $V(r_0 T)^{-\frac{1}{2}}$ must be attributed to the fact that his drops were not in fact isolated, but were connected through the conducting fluid with the source of high

Downloaded from rspa.royalsocietypublishing.org on July 13, 2012

potential, and were therefore in a distorted electric field. When expressed in the present notation Zeleny's criterion, applied to the spheroid, is

$$V(\pi T r_0)^{-\frac{1}{2}} = 4\alpha^{\frac{1}{3}} I_1. \tag{26}$$

This relation is shown in figure 2 by means of a broken curve. The difference between the two curves in figure 2 is due to Zeleny's implicit assumption that the pressure inside the drop is the same as that outside it.

Uncharged drop in a uniform field

The case is very different when the drop is uncharged and exists in a uniform electric field F. Values of $Fr_0^{\frac{1}{2}}T^{-\frac{1}{2}}$ derived from the two approximations I and II are given in table 1. The relation between $Fr_0^{\frac{1}{2}}T^{-\frac{1}{2}}$ and a/b is shown in figure 3 for approximation I, but the two approximations are so close that II is only visible over a small range near $a/b = 2$.

TABLE 1. CRITICAL VALUES OF $Fr_0^{\frac{1}{2}}T^{-\frac{1}{2}}$

I and II, approximations I and II; III, Zeleny's values.

e	a/b	I	II	III
0·00	1·000	0·000	0·000	2·363
0·20	1·020	0·473	0·46	2·363
0·50	1·154	1·136	1·14	2·308
0·75	1·512	1·564	1·575	2·159
0·80	1·666	1·610	1·622	2·093
0·85	1·898	1·625	1·635	1·992
0·88	2·105	1·608	1·623	1·916
0·90	2·294	1·583	1·588	1·839
0·92	2·550	1·537	1·542	1·747
0·95	3·202	1·406	1·424	1·564
0·98	5·025	1·092	1·086	1·153
0·99	7·092	0·856	0·849	0·889

Zeleny's criterion for the stability of drops in a uniform field when expressed in the present notation, is

$$Fr_0^{\frac{1}{2}}T^{-\frac{1}{2}} = 4\pi^{\frac{1}{2}}\alpha^{\frac{2}{3}} I_2 \tag{27}$$

and this relation is shown in figure 3 as the line III. The difference between curves I and III, which is due to Zeleny's implicit assumption that $p = 0$, is striking. It will be seen that as $Fr_0^{\frac{1}{2}}T^{-\frac{1}{2}}$ rises from zero the spheroid becomes increasingly prolate till when $a/b = 1{\cdot}9$, $Fr_0^{\frac{1}{2}}T^{-\frac{1}{2}} = 1{\cdot}625$ according to I, or 1·635 according to II, it reaches a maximum, after which it decreases. Evidently equilibrium configurations corresponding to points on the rising part of the curve are stable while those corresponding with values of $a/b > 1{\cdot}9$ are unstable.

In curve III, $Fr_0^{\frac{1}{2}}T^{-\frac{1}{2}}$ falls continuously with increase in a/b so that it is only when the pressure difference is taken into account that the spheroidal approximation can predict instability.

Comparison with experiments on the stability of drops in a uniform field

The experimental results of Wilson & Taylor (1925) namely $Fr_0^{\frac{1}{2}}T^{-\frac{1}{2}} = 1{\cdot}61 \pm 0{\cdot}04$, marked A in figure 3, agrees well with the theoretical values 1·625 according to I and 1·635 according to II. The experimental result of Macky, marked B in figure 3,

Downloaded from rspa.royalsocietypublishing.org on July 13, 2012

is about 7 % lower. The discrepancy may well be due to the fact that Macky's drops suddenly entered the electric field, dropping into it from an unelectrified region, so that they were not in a static state. They were also acted on by aerodynamic forces which would be expected in any case to create a disturbance which might well displace them from the stable to the unstable part of the curve I in figure 3 before the field reached the critical value. Wilson & Taylor's experiments on the other hand were conducted under static conditions which permitted the values of both r_0 and F to be measured accurately.

The soap films in Wilson & Taylor's experiments were initially hemispherical and stood on an earthed conducting plate. Their profiles were photographed in some cases just before the instability set in. Figure 1 of their paper (1925) is an example. Measuring the height and horizontal diameter of the bubble in this photograph I find height/diameter $= 4{\cdot}6/4{\cdot}2 = 1{\cdot}1$ so that $a/b = 2{\cdot}2$. The maximum value of F given in table 1 occurs when $a/b = 1{\cdot}9$. This is not very far from 2·2 but it is much less than the value 3 to 4 which Zeleny (1935) quotes from Macky. Since the drops could not be observed so closely in the water-dropping experiments of Macky and a close control of drop size was not possible as it was in Wilson & Taylor's experiments, the rough estimates of a/b which Macky gives cannot be regarded as measures of the critical dimensions of a drop at the moment when instability first appears.

Zeleny (1935) applied his criterion to drops in a uniform field by assuming that the drop existed with a value of $a/b = 3$ to 4. The ordinate $a/b = 3{\cdot}4$ in fact cuts Zeleny's curve III, figure 3, close to $Fr_0^{\frac{1}{2}}T^{-\frac{1}{2}} = 1{\cdot}51$ which is Macky's experimental result. Zeleny (1935) pointed out that if a/b is assumed to be between 3 and 4 his criterion for stability is satisfied and he regarded this fact as a confirmation of the correctness of his criterion as one which determines the limit of stability. The true interpretation seems to be that as a/b increases the effect of pressure on the equilibrium configuration decreases and when $a/b \sim 3{\cdot}4$ the neglect of pressure in the *equilibrium* calculation raises the calculated value of $Fr_0^{\frac{1}{2}}T^{-\frac{1}{2}}$ from 1·38 up to the value 1·51 which is close to Macky's experimental value for the limit of *stability*.

Further development of the instability

In his discussion of the stability of a charged drop Rayleigh pointed out that no instability occurs till the V reaches the value $(16\pi T r_0)^{\frac{1}{2}}$ when the instability corresponding with the Legendre function P_2 appears. For harmonics of order $n > 2$ Rayleigh shows that instability sets in when $V = (4\pi(n+2)\,r_0\,T)^{\frac{1}{2}}$, so that these instabilities can only appear when V increases beyond the point at which the P_2 instability has begun. Rayleigh evidently knew that jets develop out of the unstable ends of drops for he remarked that for great values of the charge (i.e. great values of V) the drop is unstable 'for all values of n below a certain limit, the maximum instability corresponding to a great, but still finite, value of n. Under these circumstances the liquid is thrown out in fine jets, whose fineness, however, has a limit' (Rayleigh 1896). It seems that Rayleigh's conception of the mechanics of the formation of fine jets was linked with the appearance of unstable disturbances corresponding with higher values of n for which higher values of V are required than those needed for the slightly ellipsoidal P_2 form. This appears to be contrary

Downloaded from rspa.royalsocietypublishing.org on July 13, 2012

to the experimental evidence for the jets seem to form shortly after the instability sets in without increase in the electric field. On the other hand, the ellipsoidal analysis suggests that a series of unstable ellipsoidal equilibrium states are possible in which the length increases indefinitely as the field is reduced. It seems therefore that theory might lead one to guess that when instability sets in the ellipsoidal form might persist, the drop becoming very long before it disintegrates. In fact experiments show that though it elongates to a limited extent it quickly develops an apparently conical end (figure 1) which usually oscillates and a narrow jet appears at the vertex. At this stage the ellipsoidal approximation is evidently useless and a different type of analysis is necessary.

Analysis of conditions at the point of a deformed drop

The failure of the spheroidal analysis to provide a useful model for thinking about the mechanics of the development of jets led me to approach the problem from another point of view and try to find the conditions under which a conical point could exist in equilibrium. Since the curvature of a conical surface is inversely proportional to the distance from the vertex the stress normal to it which can balance the surface tension must also be inversely proportional to distance from the vertex. Since the fluid will be assumed to be conducting the conical surface must be an equipotential, and to balance the surface tension the potential gradient there must be proportional to $R^{-\frac{1}{2}}$ where R is the radial co-ordinate.

The electric field expressed in spherical polar co-ordinates which satisfies the stress condition has potential

$$V = V_0 + AR^{\frac{1}{2}}P_{\frac{1}{2}}(\cos\theta), \tag{28}$$

where the line $\theta = 0$ or $\theta = \pi$ is the axis of the cone and $P_{\frac{1}{2}}(\cos\theta)$ is the Legendre function of order $\frac{1}{2}$. If $\theta = \theta_0$ is the conical equipotential surface where $V = V_0$

$$P_{\frac{1}{2}}(\cos\theta_0) = 0. \tag{29}$$

The function $P_{\frac{1}{2}}(\cos\theta)$ has been tabulated (Gray 1953). It has only one zero in the range $0 < \theta < \pi$ at $\theta = \theta_0 = 130{\cdot}7099°$. Since $P_{\frac{1}{2}}(\cos\theta)$ is finite and positive in the range $0 < \theta < \theta_0$ but is infinite at $\theta = \pi$ the only possible electric field which can exist in equilibrium with a conical fluid surface is that external to a cone of semi-vertical angle $\alpha = \pi - \theta_0$ or $49{\cdot}3°$.

Electric field required for conical point

The curvature of a cone of semi-vertical angle α is $\cot\alpha/R$ so that the equation of equilibrium is

$$\frac{T\cot\alpha}{R} = \frac{1}{8\pi}\left(\frac{\mathrm{d}V}{R\,\mathrm{d}\theta}\right)^2 \tag{30}$$

and from (28)

$$\frac{1}{R}\frac{\mathrm{d}V}{\mathrm{d}\theta} = AR^{-\frac{1}{2}}\left[\frac{\mathrm{d}}{\mathrm{d}\theta}P_{\frac{1}{2}}(\cos\theta)\right]_{\theta=\theta_0}. \tag{31}$$

I am indebted to Dr J. C. P. Miller for computing the value of $\mathrm{d}P_{\frac{1}{2}}(\cos\theta)/\mathrm{d}\theta$ at $\theta = \theta_0$. It is $-0{\cdot}974$, so that

$$0{\cdot}974A = 300[8\pi T\cot\alpha]^{\frac{1}{2}}. \tag{32}$$

Downloaded from rspa.royalsocietypublishing.org on July 13, 2012

The factor 300 is inserted so that electric potential is expressed in volts instead of electrostatic units. The field necessary for equilibrium with a fluid cone is therefore that represented by (28) when

$$A = 1{\cdot}432 \times 10^3 T^{\frac{1}{2}}\,\mathrm{V}\,(\mathrm{cm})^{-\frac{1}{2}}. \tag{33}$$

Experiments designed to produce a conical point under controlled conditions

It has already been pointed out that Zeleny's photographs of a disintegrating liquid surface show a thin jet emerging from an axisymmetric surface ending in a cone whose vertical angle appears to be about a right angle. In general the outline

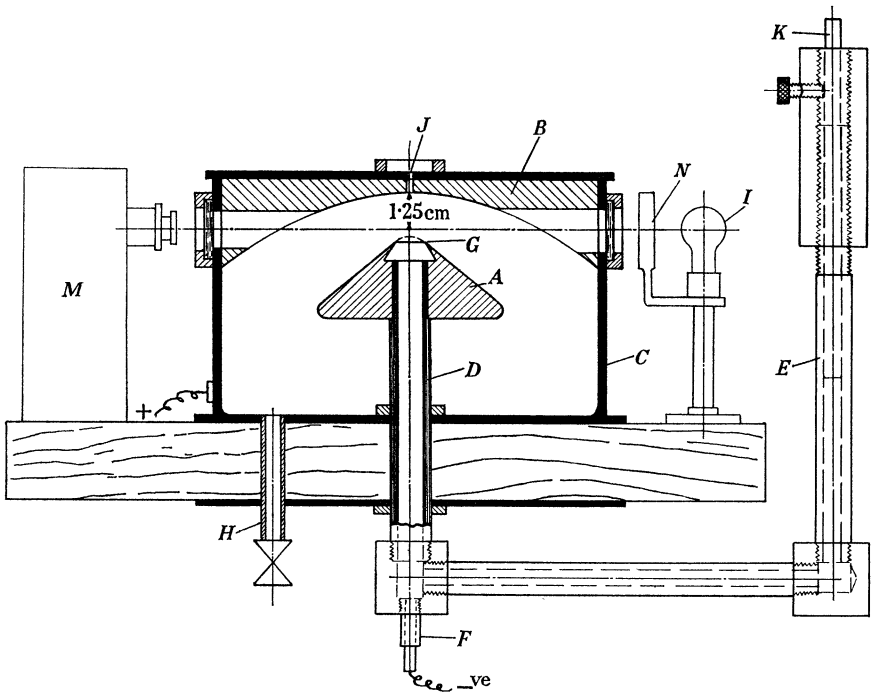

FIGURE 5. Chamber for producing field necessary for conical interface.

of the fluid surface does not consist of two straight lines so that there is some uncertainty about the angle at the vertex. To make a satisfactory experimental test of the usefulness of the analysis apparatus was constructed in which it might be possible to produce the field represented by (28) between two metallic surfaces. In the apparatus shown diagrammatically in figure 5, one surface, A, was an aluminium cone of semi-vertical angle 49·3° while the other, B, was an aluminium disk hollowed out so that its lower surface was represented by

$$R = R_0[P_{\frac{1}{2}}(\cos\theta)]^{-2}. \tag{34}$$

The value of R_0 chosen was 1·25 cm. The disk B was supported in a horizontal position with its centre 1·25 cm above the point of the cone by the cylindrical wall of a brass box, C, which was connected to earth. The cone A was supported on a non-conducting tubular pillar, D, which passed through the bottom of the box and

Downloaded from rspa.royalsocietypublishing.org on July 13, 2012

was connected with a non-conducting tubular reservoir, E. A short metal rod, F, projected through the non-conducting pillar, D, so that the cone B could be connected with a source of supply of high voltage. The object of the aluminium cone B was to ensure that the electric field near the cone could have the calculated distribution when, and if, the fluid surface assumed a conical form. The cone B was truncated so that its upper edge was a horizontal circle 1 cm diameter which could form the lower edge of a conical liquid surface if such a surface could in fact be formed. Two types of experiment were performed.

(i) A horizontal soap film was stretched across the edge G, and in order to ensure that this film was initially flat it was found necessary to undercut the aluminium so that the inner surface of the hollowed cone was a cone of semivertical angle smaller than 49·3°. For this experiment the inside of the cone was connected with the terminal F by a wire passing through the pillar D, and since the reservoir E was empty the pressure was equal on the two sides of the soap film.

(ii) The reservoir was filled with water or other conducting fluid up to the level of the edge G. A cork in the top of the tube E then prevented the level of this fluid from altering while the outer box C was filled with the non-conducting fluid, which entered through the tube H. To ensure that the interface at G was not disturbed the box was left open till the level of the non-conducting fluid rose just above G. The upper conductor A was then lowered into position the air escaping through a central vent J. The box was then filled through the tube H till the fluid appeared at J. The level of the interface could be adjusted by a non-conducting rod K moving vertically in E.

In order to observe the interface or soap film it was necessary to bore horizontal holes in the disk B. The axes of these holes passed through the point where the vertex of the aluminium cone A would have been if it had not been truncated. The holes were sealed by glass disks and photographs were taken of the profiles of the interfaces or soap films by means of a cinema camera, M. The background was a translucent screen N which was illuminated either by a steady light, I, or by a stroboscopic flashing light.

The electric field was supplied by apparatus which had been used in an experimental electron microscope and was kindly lent by Professor C. W. Oatley. The surface tension of the soap solution and that of a transformer oil/water interface were determined by the hanging drop method and the use of the calculations of Fordham (1948). In two determinations for the soap solution T was found to be 29·0 and 28·8 dyn/cm and for the oil/water interface it was 37·2.

Results

Soap film

The calculated voltage for conical equilibrium was

$$V = 1{\cdot}432 \times 10^3 (2 \times 29{\cdot}0)^{\frac{1}{2}} (1{\cdot}25)^{\frac{1}{2}} = 12{\cdot}2 \times 10^3 \text{ V}. \tag{35}$$

In view of (28) and (33) the film was stretched over the truncated top of the cone and the potential gradually raised. It showed little sign of convexity till the potential was 8000 V, it then rose with increasing voltage forming an apparently spherical cap,

Downloaded from rspa.royalsocietypublishing.org on July 13, 2012

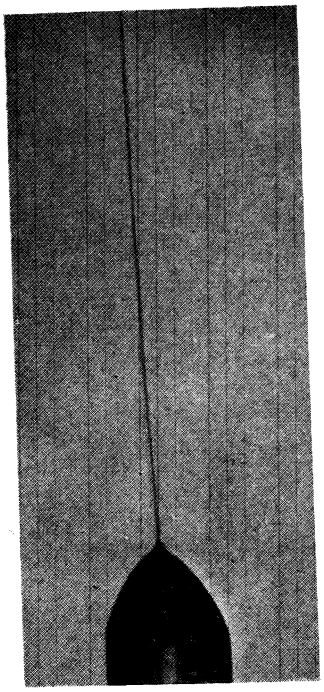

FIGURE 1

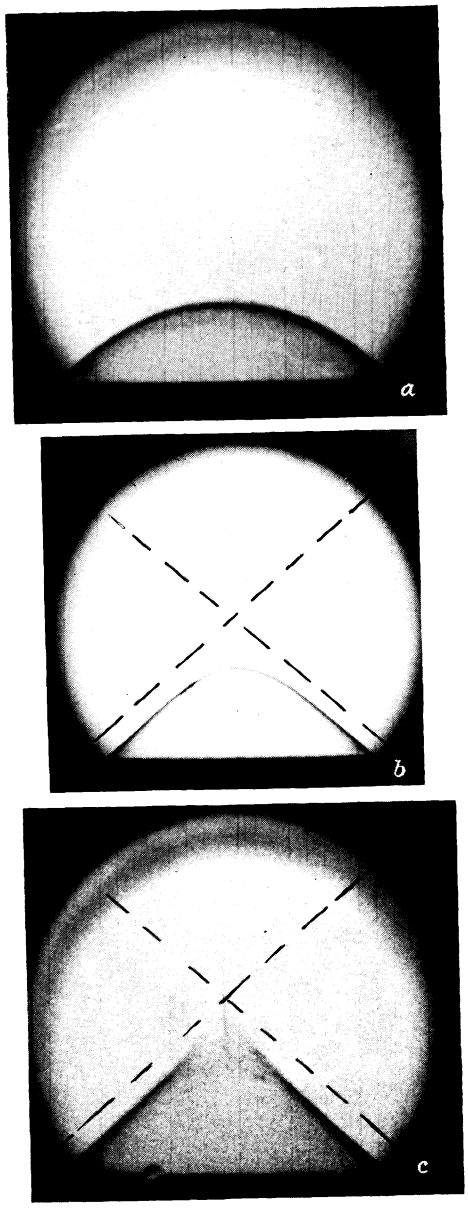

FIGURE 6

FIGURE 1. Jet of glycerine from an electrified drop (Zeleny 1917).

FIGURE 6. Soap film. Exposure time 1·6 ms. Broken lines at angle 98·6°. (*a*) Before oscillation; (*b*) oscillation beginning; (*c*) exposure covering time of jet formation.

(*Facing p.* 394)

Downloaded from rspa.royalsocietypublishing.org on July 13, 2012

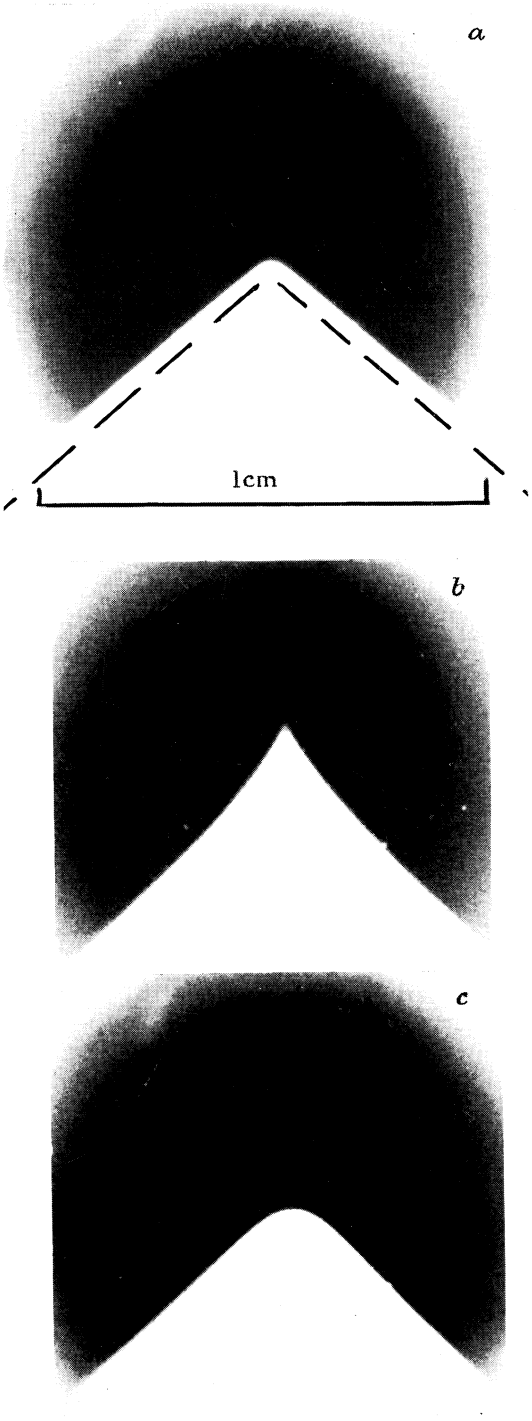

FIGURE 8

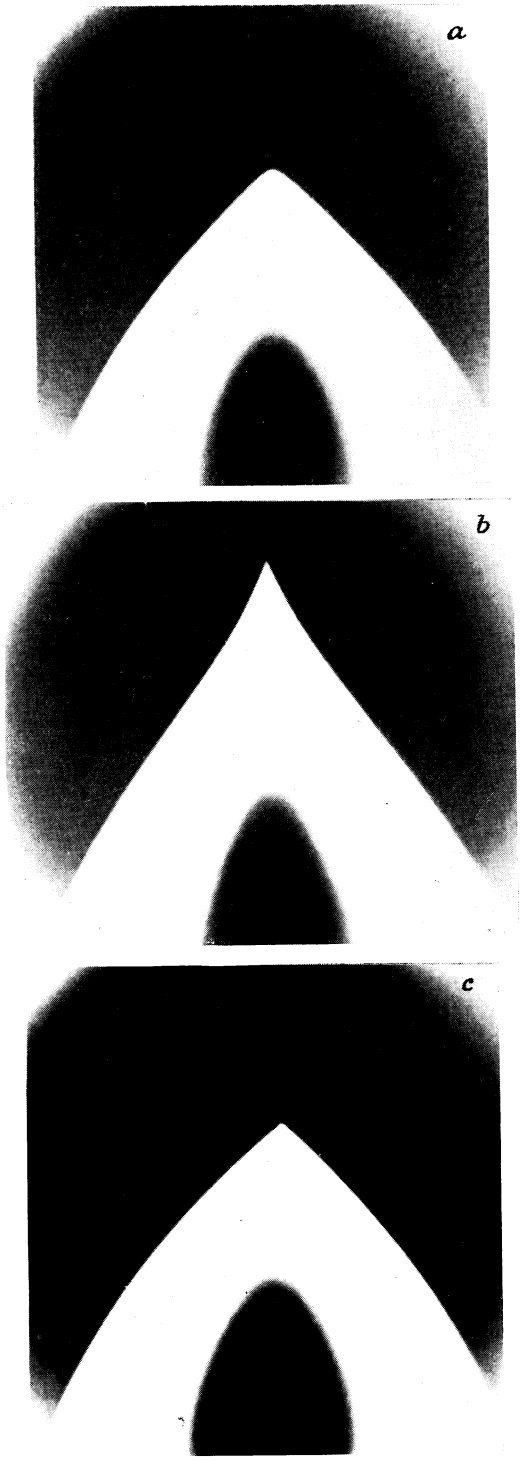

FIGURE 10

FIGURE 8. Oil/water interface. Three successive frames (1·6 ms exposures) at intervals of 1/64 s. (*a*) Before jet formation; (*b*) jet forms; (*c*) subsequent collapse. Broken lines at 98·6° (negative photo).

FIGURE 10. Oil/water interface when initial volume was in excess of requirement for 49·3° cone. (*a*) Before jet forms; (*b*) jet forms; (*c*) after jet has become detached and broken up.

Downloaded from rspa.royalsocietypublishing.org on July 13, 2012

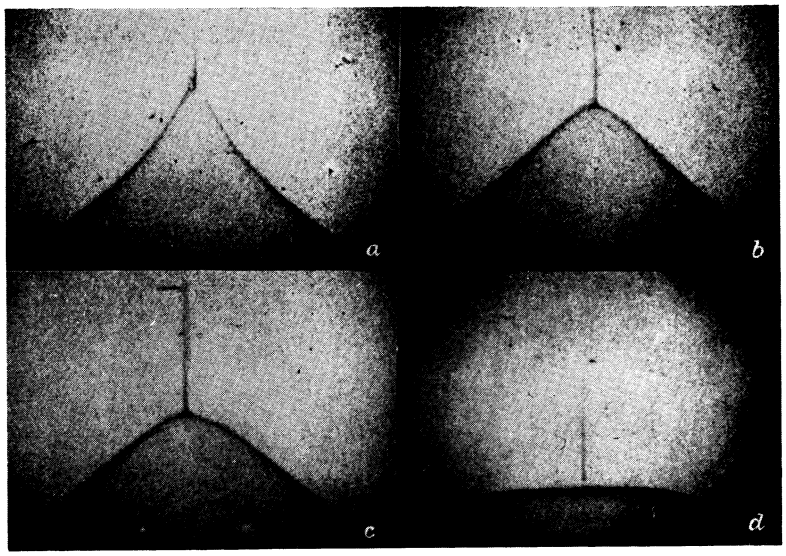

FIGURE 7. Soap film, microsecond exposures of successive stages (*a*) of jet formation; (*b*), (*c*), (*d*) subsequent collapse.

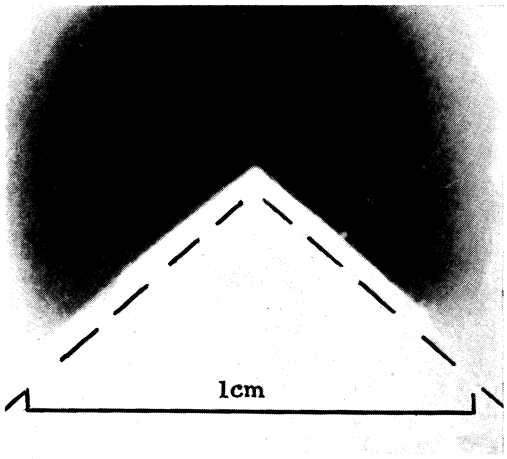

FIGURE 9. Pointed summit in oil/water interface.

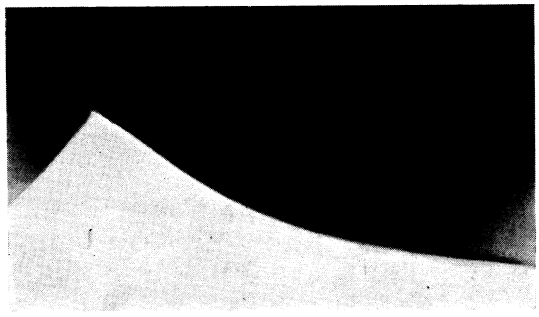

FIGURE 11. Oil/water interface when initial volume was less than needed for 49·3° cone.

Downloaded from rspa.royalsocietypublishing.org on July 13, 2012

till V reached a value which recorded as $11\frac{1}{2}$ kV it suddenly began to oscillate and at the top of each oscillation it ejected a narrow jet of soap solution. Figure 6 (*a*), plate 22, shows the film just before oscillation began. During the early unstable stages before the formation of the jet, the film rose sufficiently slowly for the camera operating at 64 frames a second to obtain clear images. The film appeared to rise at increasing speed into an imaginary conical envelope, the round top contracting as it approached the centre of the field. The semi-vertical angle of the conical part of the film was very close to the calculated equilibrium value 49·3°. Figure 6 (*b*) shows the film approaching the vertex and two straight lines at an angle 98·6° have been drawn in ink on the photograph to show how very close to the calculated equilibrium position most of the film was at that stage. Figure 6 (*c*) was taken with an exposure time of the order of 1·6 ms and during that time the film had reached its highest position, thrown out its jet and was beginning to retreat.

To obtain better definition of the formation of the jet a stroboscopic flash with duration of the order of microseconds was used. This was set to flash 100 times a second because the camera was recording at 64 frames a second and more frequent flashes would have made possible more than one exposure on the same frame. The film was in a state of violent oscillation. Figure 7 (*a*), plate 24, shows the only occasion when the jet was caught at the top of its motion in 50 ft. of film. The subsequent positions are shown in figures 7 (*b*), (*c*) and (*d*), but since these frames were taken from different parts of the film it is not certain that they can be taken as representing successive states in one oscillation. Indeed it seems likely that 7 (*b*) was very close to the top of an oscillation of smaller amplitude than those shown in 7 (*a*) and 7 (*d*). An interesting feature of the photographs is that the jet either continues to discharge when the top of the film is nearly flat at the bottom of the stroke (figure 7 (*d*)) or is pulled down by the retreating film. The latter explanation is the more likely.

The mechanics of the process seems clear. The film does not become unstable till the potential is as great or slightly greater than would be required for equilibrium if it assumed the conical form. The rapid acceleration of the top towards the point in space where the vertex of the equilibrium cone could exist indicates that the electric field is locally greater than that necessary for equilibrium, but the fact that the greater part of the film is nearly conical until the jet appears shows that away from the region close to the accelerating top of the film the field is of the form calculated for conical equilibrium. The extremely rapid acceleration which occurs just before the jet appears must be due to the fact that the extent of the region where the field differs appreciably from that of equation (28) is rapidly diminishing so that the maximum field strength at the top of the film is rapidly increasing. If similarity is preserved it must be of the same order as that at the same distance from the vertex in the field represented by (28).

The rate at which the top of the film approaches the vertex may perhaps be controlled by the inertia of the film and the air which moves with it. If h is its thickness and p its density, similarity would be preserved during the final stages if

$$ph\frac{\mathrm{d}^2R}{\mathrm{d}t^2} = -K\left(\frac{T}{R}\right), \tag{36}$$

Downloaded from rspa.royalsocietypublishing.org on July 13, 2012

where K is a constant depending on the applied potential. The velocity $\mathrm{d}R/\mathrm{d}t$ found by integrating is

$$\frac{\mathrm{d}R}{\mathrm{d}t} = -\left(\frac{2KT}{ph}\right)^{\frac{1}{2}}\left(\ln\frac{R_0}{R}\right)^{\frac{1}{2}}, \tag{37}$$

where R_0 is a constant of integration. It will be seen that it is only when R/R_0 becomes very small indeed that $\mathrm{d}R/\mathrm{d}t$ becomes large. The limiting velocity cannot be infinite as $R \to 0$ and it may well depend on the viscosity of the film. The fact that the jet, once formed, seems to remain coherent and attached to the top of the film as the latter descends, suggests that viscosity is the agent which can exert a downward force on the material of the jets and perhaps the jet is prevented from disintegrating because the electric field normal to its surface has a stabilizing influence on the varicose instability which would otherwise make it break up into small drops. On the other hand, the instability for lateral motions caused by the mutual repulsion of the charges on neighbouring parts of the jet may be prevented from developing by the stabilizing effect of the viscous tension in the jet which must exist while it is attached to the descending film. It is noticeable that the jet has always disappeared before the film begins to rise again.

It seems likely that the prime cause of the oscillation is the reduction of the field strength near the vertex which must occur when the jet, which is an equipotential surface, reduces the field strength in its neighbourhood.

The violence of the oscillation of a soap film made it desirable to experiment with interfaces where inertia and viscosity might damp the unsteady motions. In fact Zeleny's photograph, figure 1, plate 22, shows that viscosity does have that effect on jet formation.

Water/oil interface

When the interface is between a non-conducting fluid and a conducting one, gravity and viscosity as well as inertia are likely to affect the form of the interface. Attempts were made to use two fluids of the same density but practical difficulties made them unsuccessful. Experiments with transformer oil of density 0·882 and water were successful. The level of the interface was adjusted by the plunger K (figure 5). In order to give the fluid as great a chance as possible of forming a conical interface this level was adjusted in some experiments so that the volume of fluid in the space between the initially nearly spherical interface and the plane through the edge G (figure 5) was equal to that of a cone of semivertical angle 49·3° standing on the same edge.

Figure 8, plate 23, shows the interface (*a*) just before reaching the vertex, (*b*) while the jet was in action, (*c*) subsiding after the jet had stopped. These three photographs were spaced at intervals of 1/64 s and the exposure time was 1·6 ms. The oscillation was much less than for the soap film. Figure 9, plate 24, shows the summit of another oscillation just before the jet formed. The accuracy with which the semivertical angle 49·3° is attained is again remarkable. It will be noticed in figure 8 (*c*) that the jet does not follow the descending interface.

When the amount of conducting fluid above the truncated metal cone is greater than that necessary for the formation of the 49·3° cone the field necessary for conical formation cannot occur and the interface becomes ogival. Figure 10, plate 23,

Downloaded from rspa.royalsocietypublishing.org on July 13, 2012

contains three photographs at successive intervals of 1/64 s (*a*) just before jet formation, (*b*) while the jet is in action, (*c*) after the jet had stopped.

It will be seen in figure 10 (*a*) that the semi-vertical angle is rather less than 49·3° though still greater than 45°, but at the moment when the jet forms and the top of the conducting fluid is in rapid motion (figure 10 (*b*)) the angle is considerably less.

When the volume of fluid above the truncated top of the metal cone is less than that of the 49·3° cone the motion tends to become asymmetrical. Figure 11, plate 24, shows the jet which has formed under this condition and it will be seen that the interface below the jet is conical with semi-vertical angle rather greater than 45°.

Critical potential for oil/water interface

The specific inductive capacity of the transformer oil used was 2·2, and the interfacial surface tension was found to be 37 using the hanging drop method. The calculated potential for the formation of a point in the apparatus shown in figure 5 was therefore

$$V = 1{\cdot}432 \times 10^3 (37)^{\frac{1}{2}} (1{\cdot}25)^{\frac{1}{2}} (2{\cdot}2)^{-\frac{1}{2}} = 6{\cdot}5 \times 10^3 \text{ V}.$$

The measured potential was $7{\cdot}2 \times 10^3$ V for the case shown in figures 8 and 9, and $7{\cdot}6 \times 10^3$ V for that in figure 11. These are rather greater than the calculated values but imperfect insulation or molecular surface effects introduced errors into the measurements.

In conclusion I express my thanks to Professor C. W. Oatley for lending apparatus and to Mr A. D. MacEwan for help in the design of the apparatus and in carrying out the experiments.

References

Fordham, S. (1948) *Proc. Roy. Soc.* A, **194**, 1.
Gray, M. C. 1953 *Quart. App. Math.*, **11**, 311.
Jeans, J. H. 1915 *Electricity and magnetism* (3rd ed.), pp. 244–254. Cambridge University Press.
Macky, W. A. 1931 *Proc. Roy. Soc.* A, **133**, 565.
Nolan, J. J. 1926 *Proc. Roy. Irish Acad.* **37**, 28.
Rayleigh, Lord 1882 *Phil. Mag.* **14**, 184.
Rayleigh, Lord 1896 *Theory of sound.* Vol. ii, 2nd ed. (revised), p. 374.
Wilson, C. T. R. & Taylor, G. I. 1925 *Proc. Camb. Phil. Soc.* **22**, 728.
Zeleny, J. 1915 *Proc. Camb. Phil. Soc.* **18**, 71.
Zeleny, J. 1917 *Phys. Rev.* **10**, 1.
Zeleny, J. 1935 *J. Franklin Inst.* **219**, 659.

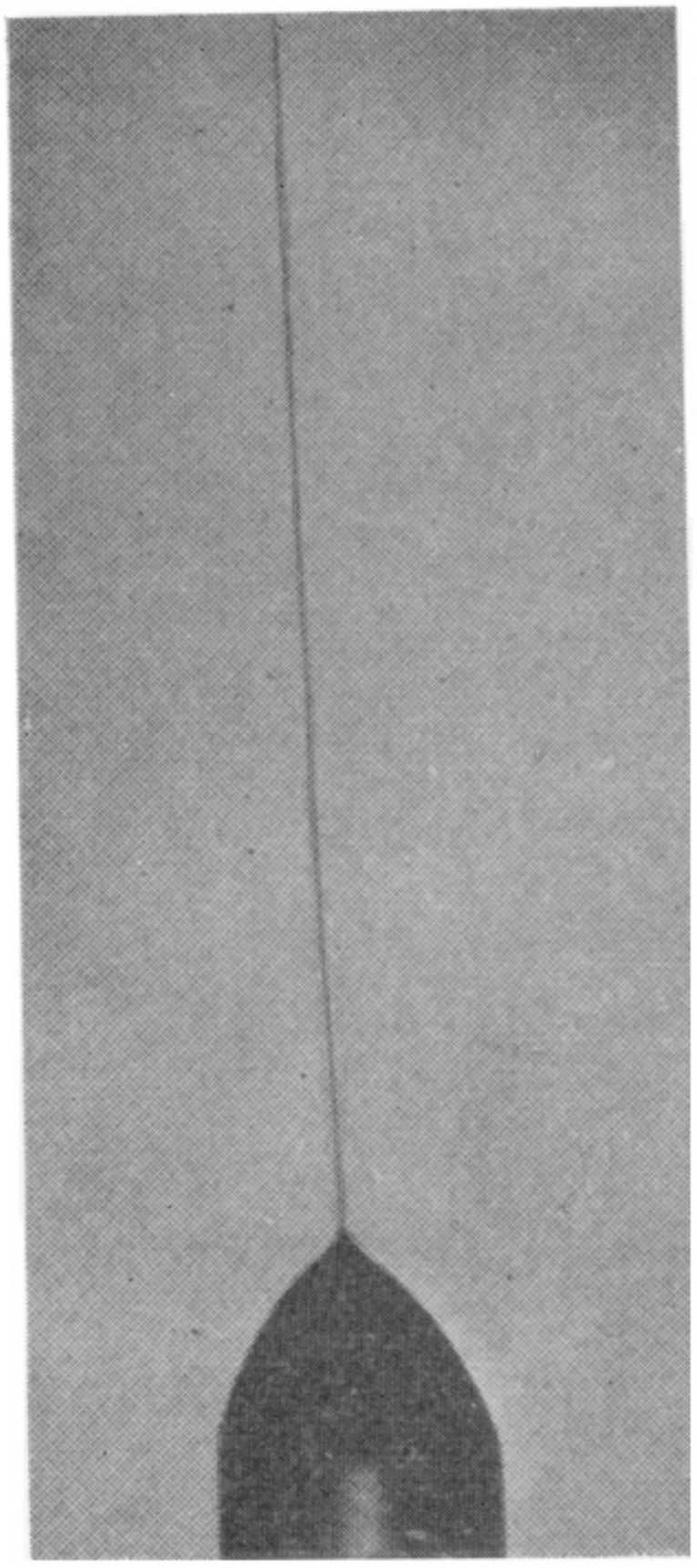

Downloaded from rspa.royalsocietypublishing.org on July 13, 2012

FIGURE 1

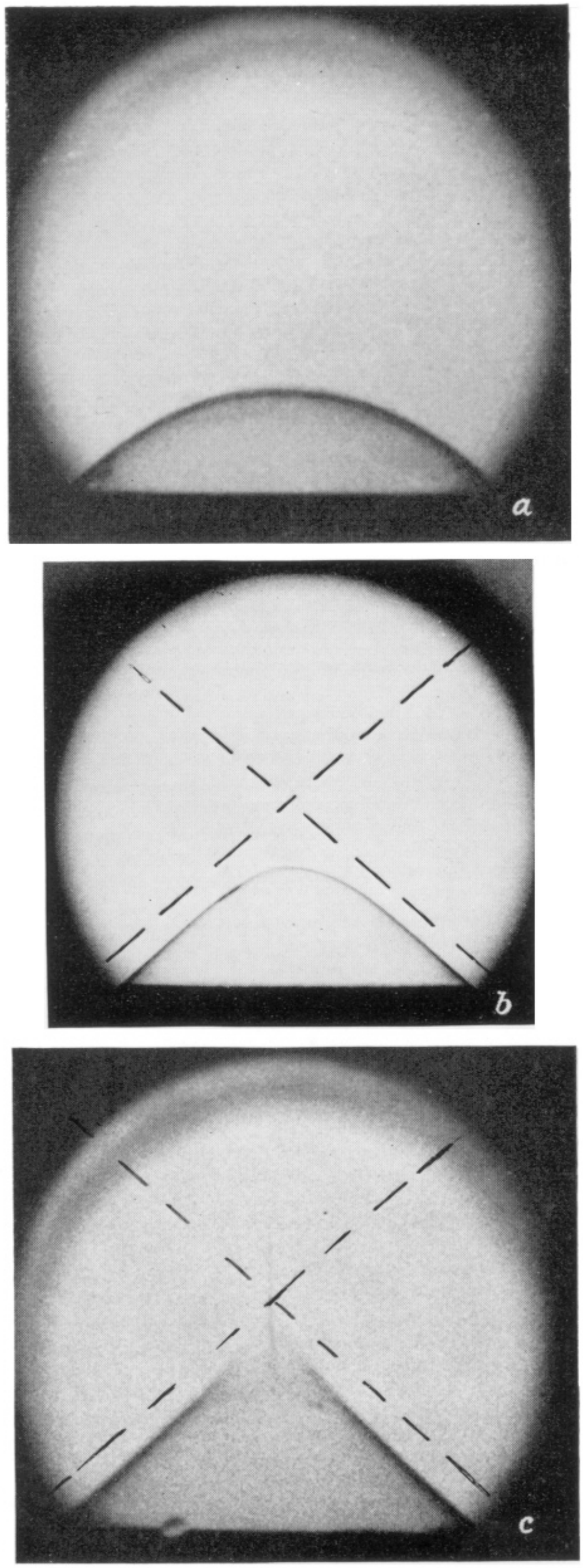

FIGURE 6

FIGURE 1. Jet of glycerine from an electrified drop (Zeleny 1917).

FIGURE 6. Soap film. Exposure time 1·6 ms. Broken lines at angle 98·6°. (*a*) Before oscillation; (*b*) oscillation beginning; (*c*) exposure covering time of jet formation.

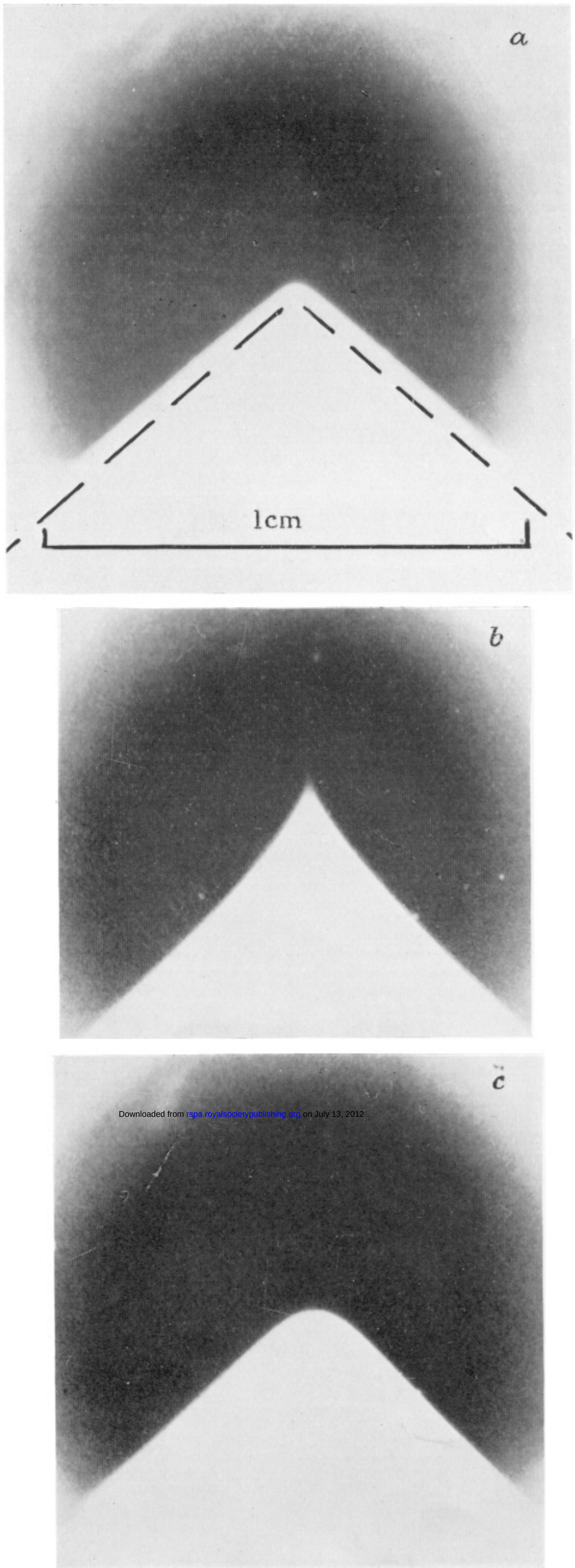

Downloaded from rspa.royalsocietypublishing.org on July 13, 2012

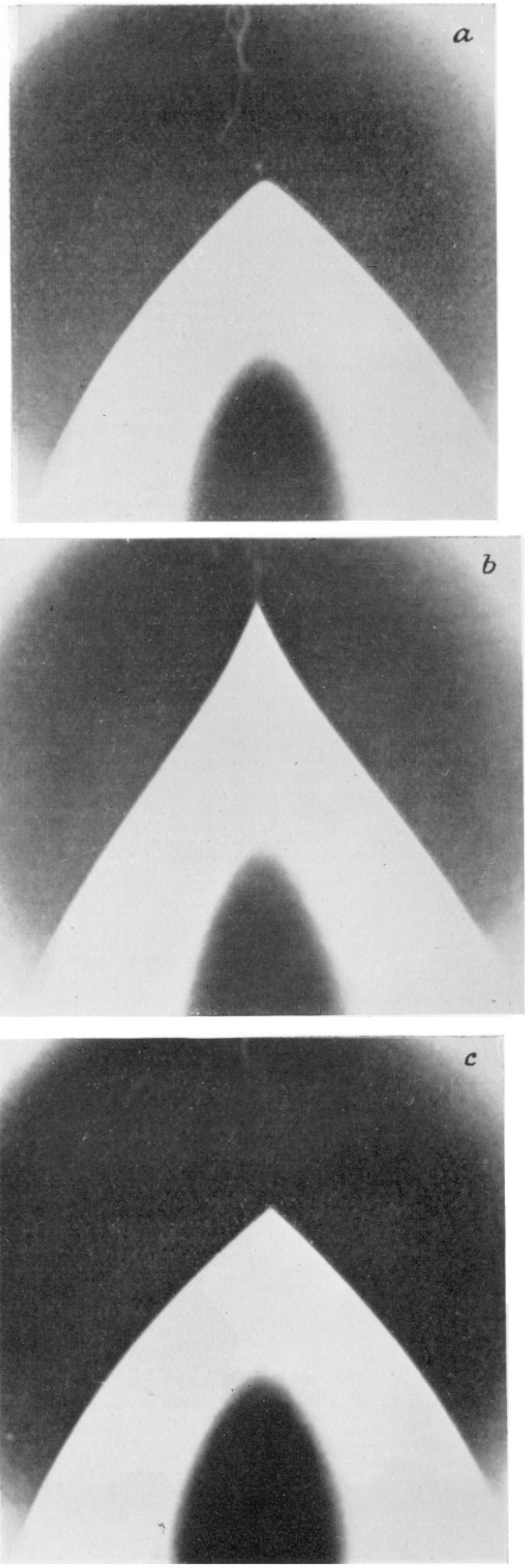

FIGURE 8

FIGURE 10

FIGURE 8. Oil/water interface. Three successive frames (1·6 ms exposures) at intervals of 1/64 s. (*a*) Before jet formation; (*b*) jet forms; (*c*) subsequent collapse. Broken lines at 98·6° (negative photo).

FIGURE 10. Oil/water interface when initial volume was in excess of requirement for 49·3° cone. (*a*) Before jet forms; (*b*) jet forms; (*c*) after jet has become detached and broken up.

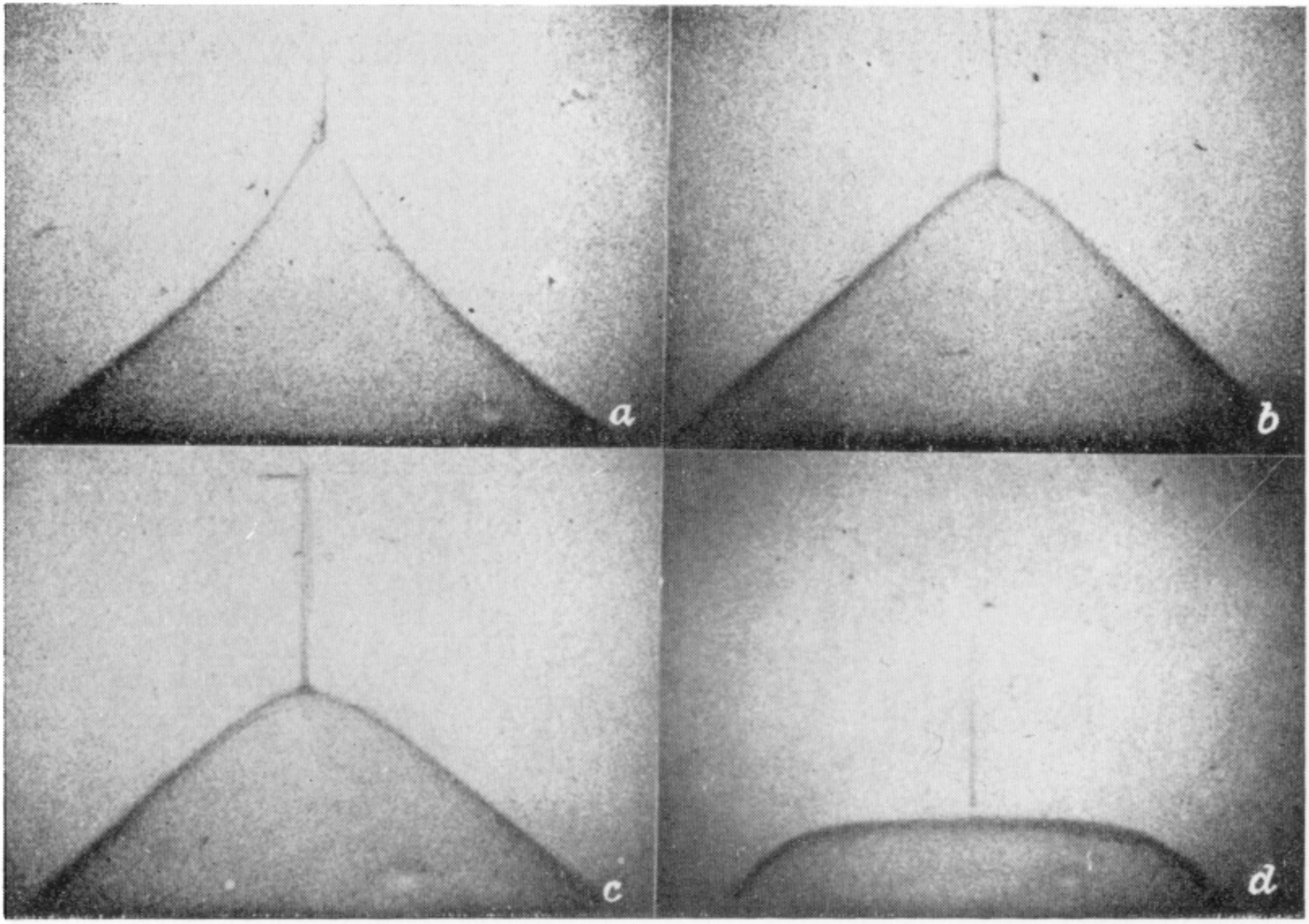

FIGURE 7. Soap film, microsecond exposures of successive stages (*a*) of jet formation; (*b*), (*c*), (*d*) subsequent collapse.

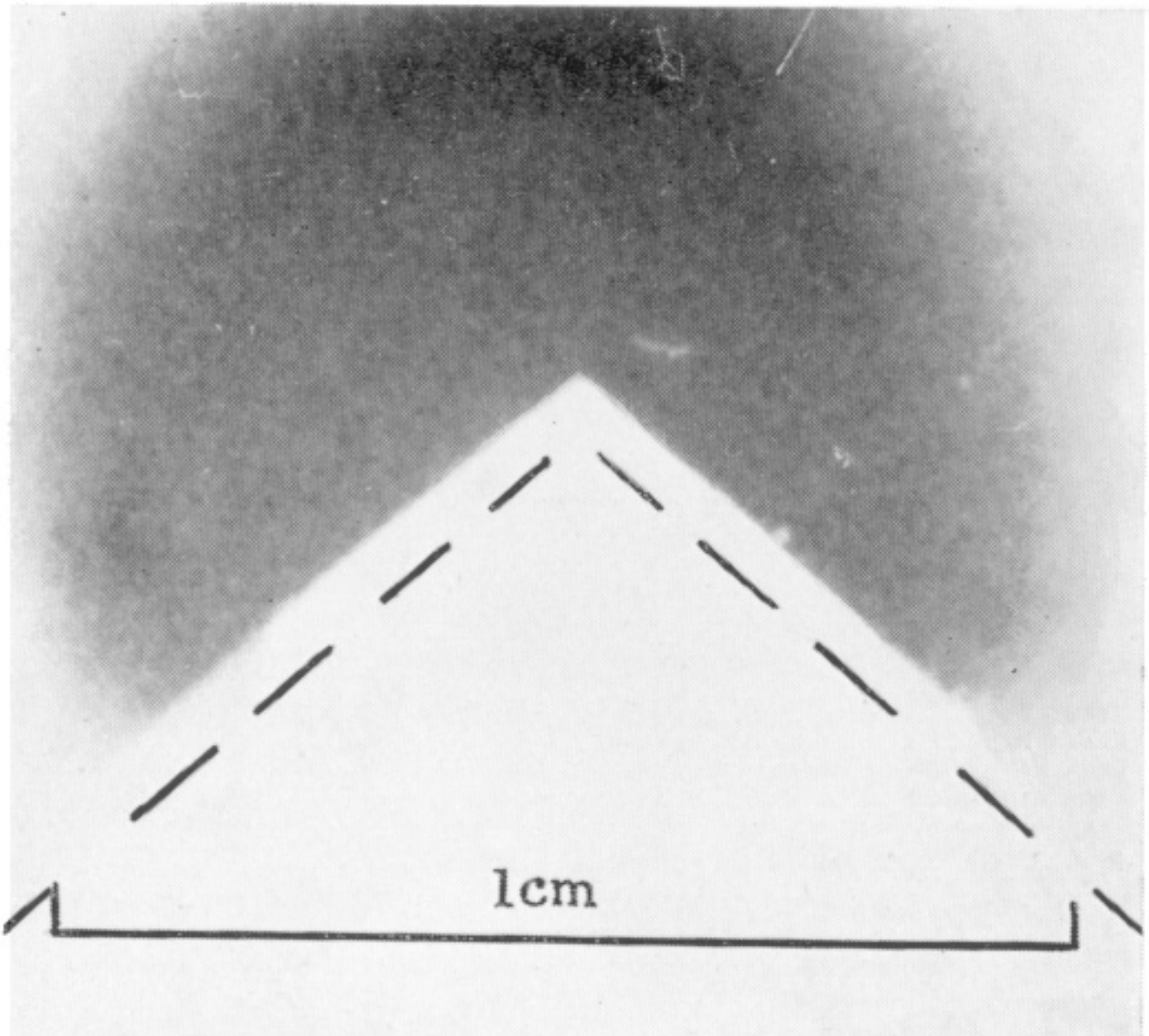

FIGURE 9. Pointed summit in oil/water interface.

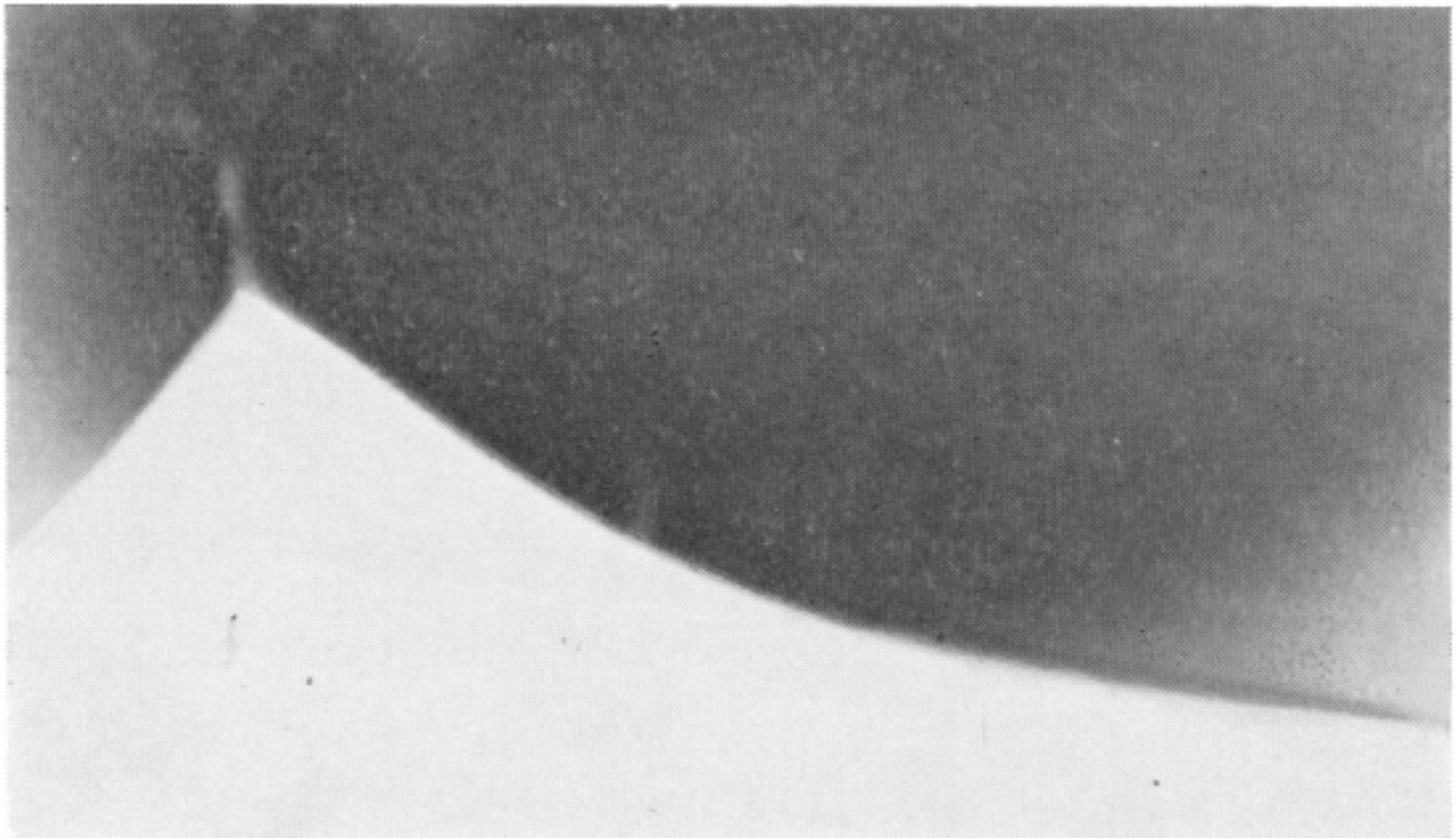

FIGURE 11. Oil/water interface when initial volume was less than needed for 49·3° cone.